CLAWAR 2019: 22nd International Conference on
Climbing and Walking Robots and the Support
Technologies for Mobile Machines,
Kuala Lumpur, Malaysia, 26-28 August 2019.
https://doi.org/10.13180/clawar.2019.26-28.08.07

PROPOSAL OF BELLOWS-INTEGRATED ROBOT FOR IMPROVING FLEXIBILITY AND SEALABILITY OF PERISTALTIC MOTION ROBOT

FUMIO ITO, TAKAHIKO KAWAGUCHI, and TARO NAKAMURA
Faculty of Science and Technology, Chuo University,
1-13-27 Kasuga, Bunkyo-Word, Tokyo 112-8551, Japan
E-mail: f_ito@bio.mech.chuo-u.ac.jp, t_Kawaguchi@bio.mech.chuo-u.ac.jp, nakamura@mech.chuo-u.ac.jp

YASUYUKI YAMADA
Faculty of Design Engineering and Technology, Tokyo Denki University,
5 Senju Asahicho, Adachi- Word, Tokyo 120-8551, Japan
E-mail: y.yamada@mail.dendai.ac.jp

Long-term use of pipes leads to increased cleaning and inspection demand. Conventional methods use long-distance inspection, which is difficult to implement due to friction along the pipe wall. Modern alternative methods, including the use of an in-pipe mobile robot, may address this issue. Nevertheless, it may be difficult for the robot to generate the necessary tractive force, especially in thin, long, and complicated pipelines. To counter such weakness, we developed a robot that mimics the peristaltic movement of an earthworm to generate a large traction force, even with small size. The robot is a bellows-integrated robot, which is characterized by high flexibility and an interior structure that does not permit the easy entrance of dust and moisture.

1. Introduction

Long-term use of pipelines creates a variety of cleaning and inspection issues. For instance, an aged and ruptured sewer pipe may result to road damage such as a depression [1]; cracks in a gas pipe destabilize gas supply [2] or; accumulated dust in the ventilation duct of a house becomes a bacteria hotbed, that when scattered indoors, will lead to health problems [3-4]. Thus, periodic or scheduled inspection and cleaning of various pipes is necessary.

Industrial endoscopes and the like are employed in current piping inspection and cleaning method for sewer or gas pipes, while an air lance, a brush with a propeller, among others, are used for cleaning of ventilation ducts installed in the house [5]. Such devices are installed with a camera and a brush that is attached at the end of the wire and air tube. The operator pushes these instruments from one end of the pipe, and then pushes in the wires or tubes behind the device, making it possible for the wire and the tool at the end of the tube to be pushed into the back of the pipe. Subsequently, inspection and cleaning can be performed in the pipe's interior.

Nevertheless, such equipment for inspection and cleaning described above may be difficult to employ in thin, complex, and long pipelines, due to the possibility of the device getting stuck to the pipe walls or receiving friction from the same walls, thereby resulting in the pushing force of the operator not transmitted into the device. Consequently, the instruments do not go through. This may be alternately resolved with the application of in-pipe mobile robots, which can be wheel-, snake-, or ciliary-vibration type, etc.—wheeled robots are likely have a complicated mechanism and a readily increasable size [6], whereas snake-like robots are capable of complex movements but require a large space for movement [7]. With this, the wheel- and snake-type robots would not be suitable for thin pipelines. Likewise, the cilia-vibration type can be moved

by a small vibration motor, but vertical and backward pipe movements could be difficult [8]. Additionally, the robot may not pass through and, therefore, is unsuitable for a long and complicated channel.

Considering these factors, we focused on the peristaltic movement of an earthworm for the in-pipe robot application. Accordingly, earthworms move by radial expansion of their body segment, thus, requiring a considerably small movement space, as well as giving a large contact area, which is ideal for a stable travel.

Some research studies have initiated various in-pipe inspections and cleaning with the peristaltic robot, which is believed to achieve long-distance inspection and cleaning [9-11]. These robots consist of a structure of connected, multiple earthworm body segments (thus, the name unit-connected robots). Nevertheless, the unit-connected robot has a long and hard flange, which compromises its flexibility and; therefore, makes its travel in complex pipes difficult. Furthermore, it has several joints that induce sealing difficulty relative to liquid and dust flow in the interior. Therefore, we proposed the peristaltic robot to mainly contain bellows, giving it the name bellows-integrated robot. Such robot is able to shorten the length of the hard flange to secure the flexibility of the whole robot. Additionally, compared to unit-connected robots, bellows-integrated robots can reduce joints, thus, making it easier to seal the inside of the robots.

Herein, we introduced the design and structure of a unit-connected robot, with an inner diameter of 50 mm, for piping inspection and cleaning. We confirmed its basic performance through an analysis of its contraction characteristics, along with some movement/travel experiments.

2. Current status of the peristaltic moving robot

2.1. *Earthworm peristaltic movement*

Figure 1 illustrates the peristaltic movement of an earthworm. Naturally, earthworms have a same-structure multiple body segments connected to each other. The operation pattern of an earthworm initiates by axial contraction of the leading body segment, followed by backward propagation of the contraction as the body segment axially extends from the head. Afterward, the axially contracted body segment simultaneously expands in the radial direction and generates friction with the contact surface. The earthworm advances using this friction.

A small space is required for such movement, which is also possible while a large contact surface is held outside; therefore, it is suitable for long-distance movement in a complex capillary.

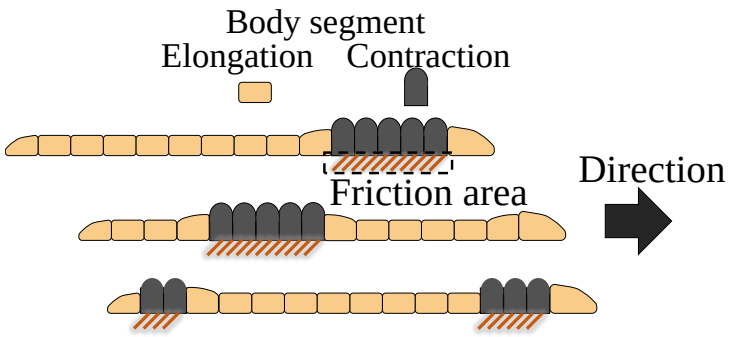

Figure 1 States of an earthworm movement

2.2. *Unit-connected robot*

We developed a robot that can mimic the peristaltic movement of earthworms through connecting multiple units that move in the same way as the earthworm's body segment. Figure 2 shows the appearance of a unit-connected robot for the purpose of inspection and cleaning inside a tube with an inner diameter of 50 mm, whereas Fig. 3 displays the appearance of the unit, which uses an axial-fiber reinforced artificial muscle (referred to as artificial muscle herein). Upon the injection of air pressure, the unit expands in the radial direction, while it contracts in the axial direction [12]. By connecting the multiple units and applying air pressure sequentially from the unit at the top of the traveling direction, the robot propels toward a peristaltic motion.

Fig. 4 shows the components of the unit. It is configured from a combination of Figs. 4(a) to 4(e). In simple terms, a peristaltic robot is constructed by connecting fabricated multiple units. As mentioned earlier, this unit loses its flexibility due to the hard and long flange, and sealing the interior becomes difficult as the joints of the robot are increased. For this reason, we proposed an improvement for both flexibility and sealability.

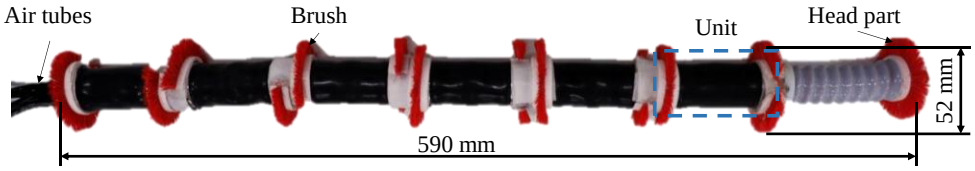

Figure 2 External view of the unit-connected robot

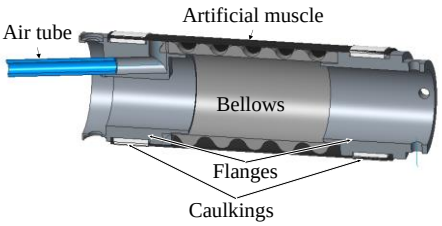

Figure 3 A unit of the unit-connected robot

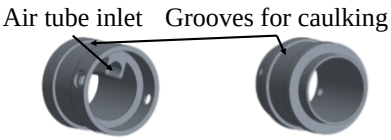

(a) The unit flange

(b) Bellows

(c) Artificial muscle

(d) Caulking tool

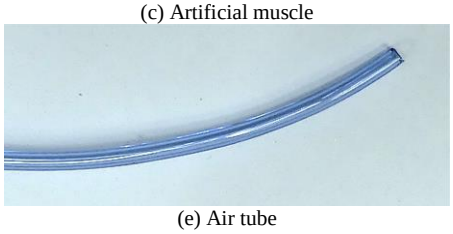

(e) Air tube

Figure 4 Unit components

3. Outline of the bellows-integrated peristaltic moving robot

3.1. *Bellows-integrated peristaltic robot*

Figure 5 provides an external view of the bellows-integrated robot, which is aimed at improving the flexibility and sealability of the peristaltic robot, and which consists of an artificial segment, head, air tube, and brush. Through the application of air pressure, each segment expands in the radial direction and contracts in the axial direction. In particular, as air pressure is applied sequentially from the segment at the top of the traveling direction, it is propelled in the pipe, while performing peristaltic motion.

The brush between the segments rubs against the inner wall as it travel-cleans through the pipe. Moreover, with camera attached to the head, in-pipe inspection is possible.

Table 1 shows a comparison of the weight and total length of the bellows-integrated and unit-connected robots. Notice that the former has less weight and shorter length, and is easier to handle than the latter.

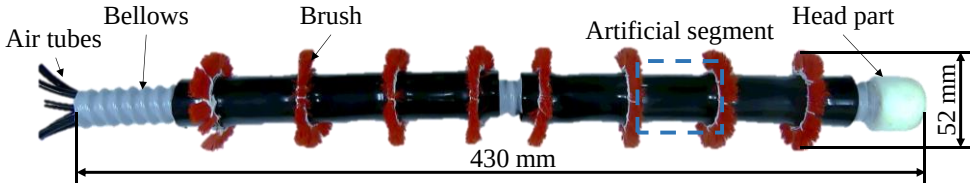

Figure 5 External view of a bellows-integrated peristaltic robot

Table 1 Dimensions of two in-pipe robots

	Weight [g]	Length [mm]
Bellows integrated type	145	430
Unit connected type	520	590

3.2. *Motion pattern and theoretical speed*

Figure 6 shows the flow of one cycle of the bellows-integrated robot. It has the same theoretical speed of travel as that of the unit-connected robot, given by Eq. (1), used conventionally. Table 2 lists the parameters applicable for Eq. (1). Thus, the theoretical speed of a peristaltic robot can be calculated by: (movement amount per cycle)/(time per cycle).

$$V = \frac{rlsn}{Nt} \tag{1}$$

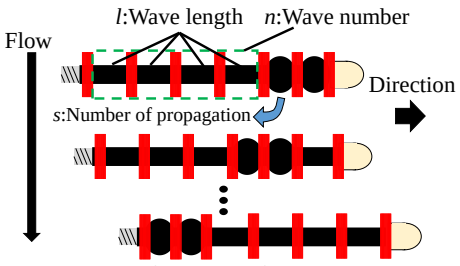

Figure 6 Flow of one cycle of a peristaltic robot

Table 2 Parameters for the equation of velocity of the peristaltic robot

V	Robot speed [mm/s]
r	Amount of contraction of one segument [mm]
t	Moving cycle [s]
N	Number of units [-]
l	Wave length [mm]
n	Wave number (Number of extending unit groups) [-]
s	Number of propagation [-]

3.3. *Control system*

Figure 7 illustrates the control system of the proposed robot. Air pressure applied to each segment is controlled by an Arduino Mega 2560. A D/A converter converts the digital voltage from the Arduino into an analog voltage, which it then sends to the proportional solenoid valve. Subsequently, the air pressure of the compressor is applied to each segment via a manifold and a proportional solenoid valve, in proportion to the valve's amount of analog voltage input. In this manner, each segment can be expanded and contracted independently.

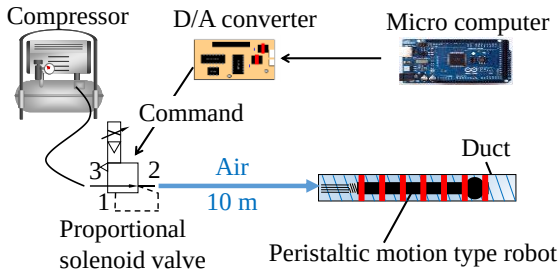

Figure 7 Control system of the bellows-integrated peristaltic motion robot

4. Design of the bellows-integrated peristaltic motion robot

4.1. *Length between each segment*

Figure 8 shows a geometrical model for determining the length between each segment, while Table 3 provides the parameters used in this model. The artificial muscle is assumed to expand in a circular pattern. Equation (2) describes the governing calculation for determining the length between each segment.

The initial outer diameter of the artificial muscle is set to 25 mm in consideration of the space through which the air tube passes inside the robot. On this scale, the maximum expansion diameter is set to 55 mm, which is equal to or greater than the inner diameter of the pipe, sufficient for gripping the pipe of a target 50-mm diameter. Using Eq. (2), the length between segments is 47 mm.

$$L = \frac{d_m - d_o}{1 - \alpha} \tag{2}$$

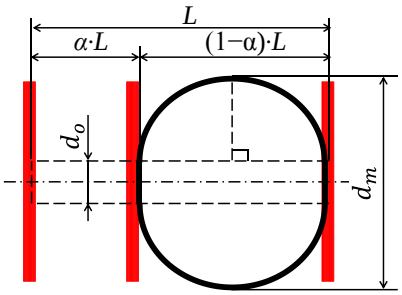

Figure 8 A model illustrating the calculation of the segment length

Table 3 Parameters of the segment length calculation model

L	Segment length [mm]
d_0	Non expansion outer diameter of artificial muscle [mm]
d_m	Max expansion outer diameter of artificial muscle [mm]
α (≈0.36)	Contraction rate [−]

4.2. *Structural design*

Figure 9 shows the flange of the bellows-integrated robot. It is a cylindrical structure of the same shape and can be screwed directly into the bellows. The flange required to fix an artificial muscle is short and gives the robot the desired flexibility.

In this study, we fabricated a bellows-integrated peristaltic robot with a segment number N of 6 in consideration of the number of air tubes passed inside it. The succeeding section discusses the measurement procedure for the pressure characteristics of the robot.

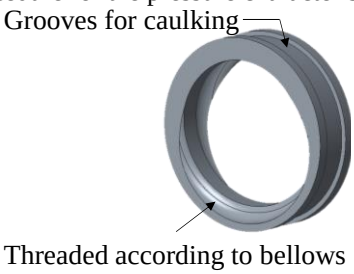

Figure 9 A flange of bellows-integrated peristaltic robot

5. Characteristics of segment contraction

Each segment of the proposed robot has the same structure as each unit of the unit-connected robot, implying the same pressure response. Therefore, the response characteristics of the same unit were used as the response of each segment, with the corresponding inner pipe diameter and the artificial muscle and bellows being the same. Figure 10 shows the measurement method. Each unit is placed in the duct, with one end fixed, and the other end in motion. With this scheme, the displacement performed by the movable part as air pressure is applied to each unit is measured by a distance sensor. Additionally, let contraction time be the time until the contraction amount reaches 95% of the final value from the time air pressure is applied to each unit. After application of air pressure, the exhaust command is issued once the amount of contraction reaches the final value. Subsequently, let extension time be the time until the extension amount reaches 95% of the final value. Herein, the applied pressure is 0.20 MPa, which is the lowest pressure that can hold a pipe with an inner diameter of 50 mm.

Figure 11 shows the measurement results, and Table 4 the contraction and elongation time. With reference to Table 3, the parameters of the earthworm robot are s = 1, n = 4, r = 9.8 mm, and t = 0.75 s, for a theoretical speed of 8.7 mm/s following Eq. (1). The succeeding chapter will discuss a comparison of the speeds of the bellows-integrated and unit-connected robots.

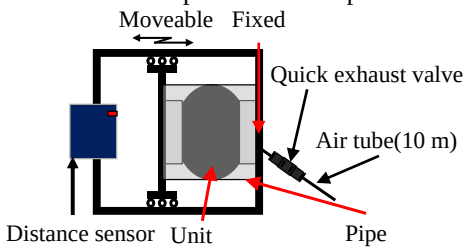

Figure 10 Experimental conditions for measurement of the contraction characteristics

Table 4 Contraction time and extension time

Contraction time [s]	Elongation time [s]
0.75	0.47

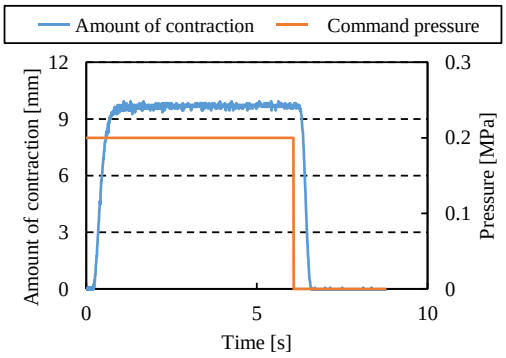

Figure 11 Pressure response waveform of a unit

6. Robot running test

We conducted an experiment measuring the travel speed of both the bellows-integrated robot and the unit-connected robot. Each robot was placed in a straight, acrylic pipe, was run 0.5 m three times, and its average speed was measured. The applied pressure was 0.20 MPa; the air tube was 10 m long and; the operation pattern was the same as the parameters for calculation of the theoretical velocity. Figures 12 and 13 describe the travel pattern of the bellows-integrated and unit-connected robots, respectively. Figure 14 shows the experimental results.

Based on Figure 14, the running speed of each robot was slower than the theoretical speed, which may be attributed to the friction resistance generated in the tube and pulled by the robot, along with the resistance caused by the friction generated in the brush mounted around the robot. Moreover, the travel speed of the bellows-integrated robot was slower than that of the unit-connected robot, which was expected because the spring constant of former is lower than that latter, resulting to reduced pushing force.

It is believed that this speed reduction can be reduced by a selection of the bellows. In the future, we will investigate the types of bellows that can ensure the flexibility of the robot as it generates the pushing force.

Figure 12 State of the bellows-integrated robot

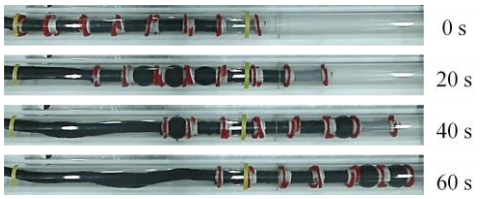

Figure 13 State of the unit-connected robot

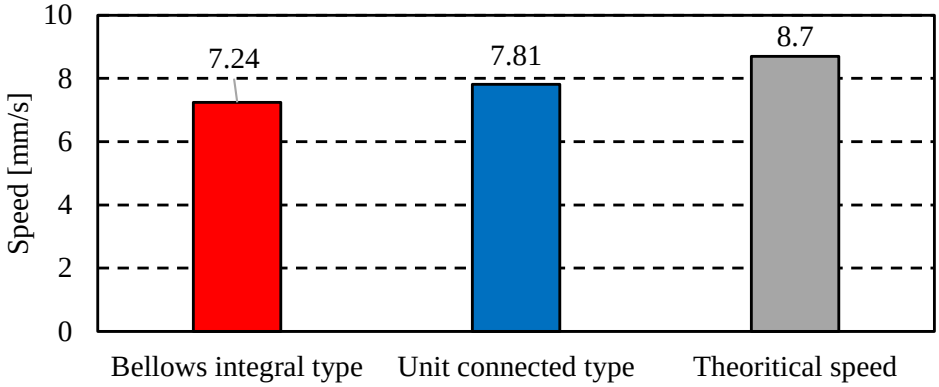

Figure 14 Speed comparison of each robot

7. Conclusion

We proposed a bellows-integrated robot aimed at improving its flexibility and sealability for in-pipe inspection and cleaning. First, we confirmed its running performance through contraction response and running test, which we compared to those of the unit-connected robot afterward. As expected, the proposed robot improved in flexibility and sealing without its travel speed being reduced.

In the future, we will select a bellows suitable for the structure of this robot, as well as examine the performance in both the curved pipe passage and long-distance travel.

References

1. H. Uchida and K. Ishii, “Basic Research on Crack Detection for Sewer Pipe Inspection Robot Using Image Processing,” The Proceedings of JSME annual Conference on Robotics and Mechatronics (Robomec). (2009).
2. S. Yoda, Y. Wakibe and Y, “Inspection methods of piping,” *Bull Soc Sea Water Sci.* **68**, 57–62 (2014) (in Japanese).
3. B. Zhou, B. Zhao and Z. Ta, “How Particle Resuspension from Inner Surfaces of Ventilation Ducts Affects Indoor Air Quality–A Modeling Analysis,” *Aerosol Sci Technol.* 45, 996–1009 (2011).
4. H. Yoshino, K. Amano, M. Matsumoto, K. Netsu, K. Ikeda, A. Nozaki, K. Kakuta, S. Hojo and S. Ishikawa, “Long-termed Field Survey of Indoor Air Quality and Health Hazards in Sick House*,” J Asian Archit Build*. **3**, 297–303 (2004).
5. O. Winton Co., Ltd. Home Page.16 Jan 2017. OsakaWintonCo. Ltd. http:www.osaka winton.co.jp/en/air_conditioning/
6. S. U. Yang, H. M. Kim, J. S. Suh, Y. S. Choi, H. M. Mun, C. M. Park, H. Moon and H. R. Choi, "Novel Robot Mechanism Capable of 3D Differential Driving Inside Pipelines,” *2014 IEEE/RSJ International Conference on Intelligent Robots and Systems (IROS 2014)* September 14–18, 2014, Chicago, IL, USA
7. H. Amir, M. Heidari, R. Mehrandezh, et al, Dynamic analysis and human analogous control of a pipe crawling robot,” *Proceedings of IEEE/RSJ International Conference on Intelligent Robots and Systems*; Oct 10–15, 2009, Missouri (TX): St. Louis, 733–740.
8. K. Masashi, H. Kazunari, I. Kazuya, et al, “Development of an active scope camera driven by ciliary vibration mechanism,” *Proceedings of the 12th ROBOTICS symposia*, Nov 8–9, 2007, Monterrey, 460–465.
9. M. Kamata, S. Yamazaki, Y. Tanise, Y. Yamada and T. Nakamura, “Morphological change in peristaltic crawling motion of a narrow pipe inspection robot inspired by earthworm’s locomotion, *Advanced Robotics.* 386-397 (2017).
10. R. Ishikawa, T. Tomita, Y. Yamada and T. Nakamura, “Development of a Peristaltic Crawling Robot for Long-distance Complex Line Sewer Pipe Inspections,” *2016 IEEE International Conference on Advanced Intelligent Mechatronics (AIM)*, Banff, Alberta, Canada, July 12–15, 2016
11. Y. Tanise, K. Taniguchi, S. Yamazaki, M. Kamata, Y. Yamada and T. Nakamura, “Development of an air duct cleaning robot for housing based on peristaltic crawling motion,” *2017 IEEE International Conference on Advanced Intelligent Mechatronics (AIM)*, Sheraton Arabella Park Hotel, Munich, Germany, July 3–7, 2017.
12. T. Nakamura and H. Shinohara, "Position and force control based on mathematical models of pneumatic artificial muscles reinforced by straight glass fibers,” *Proc. of IEEE Int. Conf. on Robotics and Automation ICRA*, pp. 4361–66 (2007).